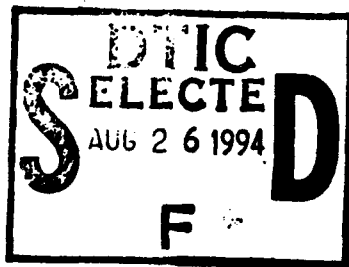


AD-A283 740

F			AGE	
1 AGENCY USE ONLY		2 REPORT DATE SEPT 93		3 TYPE/DATES COVERED
4 TITLE AND SUBTITLE THE MEASUREMENT OF DYNAMIC STRUCTURAL STRESSES IN A LIGHT ARMOUNED VEHICLE			5 FUNDING NUMBERS	
6 AUTHOR S J CIMPOERU			8 PERFORMING ORG. REPORT NO	
7 FORMING ORG NAMES/ADDRESSES DEFENCE SCIENCE AND TECHNOLOGY ORGANIZATION, MATERIALS RESEARCH LABORATORY, PO BOX 50, ASCOT VALE VICTORIA 3032 AUSTRALIA				
09 SPONSORING/MONITORING AGENCY NAMES AND ADDRESSES				
11 SUPPLEMENTARY NOTES				
12 DISTRIBUTION/AVAILABILITY STATEMENT DISTRIBUTION STATEMENT A			12B DISTRIBUTION CODE	
13 ABSTRACT (MAX 200 WORDS): THE MEASUREMENT OF DYANAMIC STRESSES IN THE STRUCTURAL ARMOUR OF AN LAV-25 LIGHT ARMOUNED VEHICLE IS DESCRIBED ALONG WITH A PRELIMINARY ANALYSIS OF THE DATA. STRESSES WERE MEASURED USING STRAIN GAUGE ROSETTES MOUNTED AT CRITICAL LOCATIONS AS THE VEHICLE TRAVERSED OVER A RANGE OF TERRAIN TYPES. THE MEAN, ROOT MEAN SQUARE AND MAXIMUM EFFECTIVE STRESSES FOR SELECTED STRAIN GAUGE LOCATIONS ARE COMPARED FOR THE DIFFERENT TERRAIN TYPES. OVERALL, THE MEASURED OPERATING STRESSES WILL PROVIDE THE DYNAMAIC STRESS DATA ESSENTIAL FOR A CORRECT LABORATORY SIMULATION OF THE SERVICE ENVIRONMENT OF AN LAV-25.				
14 SUBJECT TERMS			15 NUMBER OF PAGES 7	
			16 PRICE CODE	
17 SECURITY CLASS.REPORT UNCLASSIFIED	18 SEC CLASS PAGE UNCLASSIFIED	19 SEC CLASS ABST. UNCLASS	20 LIMITATION OF ABSTRACT	



This document has been approved for public release and sale; its distribution is unlimited.

98 **94-27219**


94 8 25 053

5th Australian Aeronautical Conference

13-15 September 1993

Regent Hotel, Melbourne, Australia

Accession For	
NTIS CRA&I	<input checked="" type="checkbox"/>
DTIC TAB	<input type="checkbox"/>
Unannounced	<input type="checkbox"/>
Justification	
By	
Distribution/	
Availability Codes	
Dist	Avail and/or Special
A-1	20

DTIC QUALITY INSPECTED 1

The Measurement of Dynamic Structural Stresses in a Light Armoured Vehicle

S.J. CIMPOERU, B.E., M.Eng.Sci., GradIEAust,

Ship Structures and Materials Division, Materials Research Laboratory, DSTO Australia.

SUMMARY The measurement of dynamic stresses in the structural armour of an LAV-25 light armoured vehicle is described along with a preliminary analysis of the data. Stresses were measured using strain gauge rosettes mounted at critical locations as the vehicle traversed over a range of terrain types. The mean, root mean square and maximum effective stresses for selected strain gauge locations are compared for the different terrain types. Overall, the measured operating stresses will provide the dynamic stress data essential for a correct laboratory simulation of the service environment of an LAV-25.

1. INTRODUCTION

The LAV-25 is an eight wheeled light armoured fighting vehicle which is armed with a 25 mm chain gun, mounted in a revolving turret, Fig 1. Vehicles such as these are being acquired by the Australian Army for reconnaissance operations in Northern Australia. A high hardness steel that has been quenched and tempered is used for the construction of its structural armour. This class of material has the potential to develop cracks under certain environmental and service conditions. Since such cracking may affect both the structural integrity and ballistic protection of these vehicles, a research program was initiated to better understand and develop effective solutions to minimise any through-life cracking problems which may arise. This is a difficult problem as such cracking can develop as a result of careless vehicle fabrication, i.e. loose material specifications as well as poor plate cutting and welding procedures. Moreover, such cracking can also be exacerbated by fatigue loading and stress corrosion, especially in the presence of high residual stresses. Part of the research program (the current paper) involved the measurement of the in-service stresses in the structural armour of an LAV-25 as it traversed a range of terrain types at the Australian Army's Monegetta proving ground, namely, bitumen, corrugated, and gravel roads together with a cross-country course. As well as providing insight into the magnitude of the dynamic stresses at various critical locations, this data will be used in conjunction with

separately measured internal stress data to drive servo-hydraulic fatigue testing machines so that realistic fatigue and stress-corrosion testing can be performed as part of an overall study into the cracking problem.

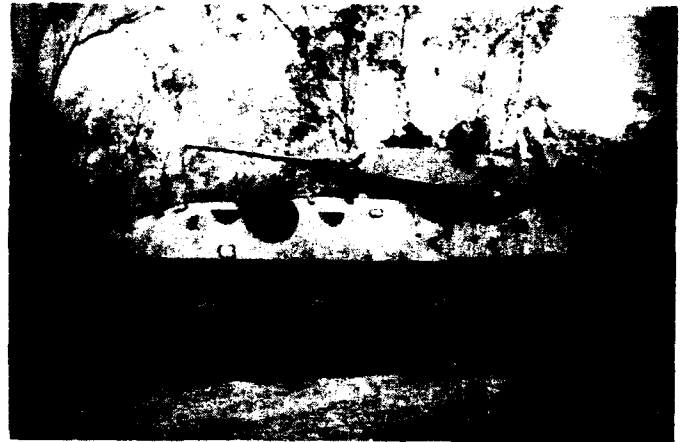


Figure 1: An LAV-25 vehicle in the field.

2. EXPERIMENTAL

2.1. Proving Ground Course

The test vehicle was trialed by being driven around a selected test circuit at the Monegetta Proving Ground of the Australian Army Engineering Development Establishment. Table 1 details the component sections of the test circuit. The characteristics of each of the terrain types are self-explanatory, except for the 'Herringbone' Ripple-Bar Course, Fig. 2. This latter terrain is used to simulate the corrugation ripples that are often found in outback roads. The

herringbone ripple-bar pattern simulated roads with corrugations that are off-set from each wheel.

Terrain	Characteristics	Distance
First Class Road	normal bitumen road	3.6 km
Herringbone Ripple-Bar Rough Course	regularly spaced herringbone concrete ripples	209 m
Second Class Road	a graded gravel road	4.5 km
Cross-Country Course	an ungraded dirt track with large pot-holes	1.4 km

Table 1: Characteristics of the test circuit.



Figure 2: Segment of Herringbone Ripple-Bar Course at Monegetta. The vehicle traversed this course from the left to right.

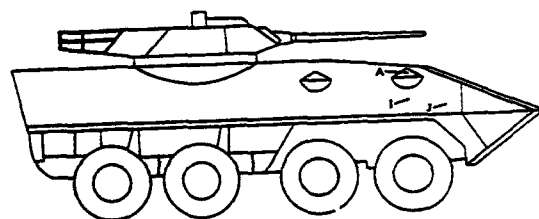
The trial required a number of laps or runs around the test circuit because only 6 data channels were able to be recorded at any one time. The vehicle was driven at maximum safe speed over each of the circuit sections. This ensured that the vehicle travelled at a repeatable speed over each section of the course and that the stresses in the vehicle were maximised, impact loads being speed dependent. The vehicle was trialed at combat mass with no axle load exceeding the recommended mass limit. The tyre pressures were set to 426 kPa (62 p.s.i.) and checked at the start of each day.

A micro-video camera was also employed for some of the runs to assist in relating vehicle stresses back to the terrain. The camera was off-set from the vehicle to record both the

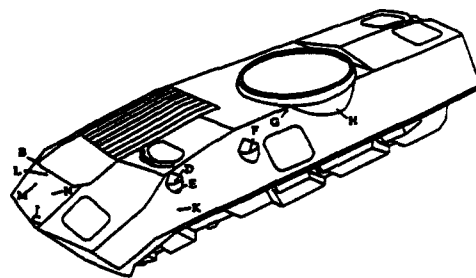
terrain directly ahead of the vehicle and the response of the suspension.

2.2. Strain Gauge Installation

Twelve strain gauge rosettes were mounted at potential cracking sites on the hull of the test vehicle. These locations were chosen after considering likely stress concentration sites as well as crack locations in similar vehicles. Fig. 3(a) and (b) depict the gauge locations. The trial was conducted in two phases so that the strain data from eight initially placed gauges (Rosettes A to H) could be inspected and used to help determine the locations for the final six gauges (Rosettes I to N). This procedure also minimised the possibility of placing the majority of the gauges in low stressed regions of the hull.



(a)



(b)

Figure 3: Strain gauge rosette locations on the test vehicle.

Forty-five degree 350 Ω rosettes, type Micro Measurements CEA-06-250UR-350 (6.4 mm grid gauge length), were used for all measurements except for Rosette L and M which were of the CEA-06-125UR-350 type (3.2 mm grid gauge length).

All gauges were planar type three element rosettes, chosen for ease of both leadwire attachment and application to curved surfaces. However, the individual grids of these rosettes were adjacent rather than superimposed on exactly the same locations. These rosettes therefore measured an 'average' strain reading over a finite area, larger than just the gauge length of an individual grid. While this is a disadvantage with high strain gradients, this factor was not considered to lead to significant errors in the current application.

Each rosette was waterproofed after application to prevent moisture ingress which would otherwise reduce the insulation resistance to ground, leading to noise as well as gauge instability and drift (1). Firstly two thin clear coats of M-Coat A™ were applied shortly after gauge application. Short jumper leads were then soldered to connect the terminals of each rosette to bondable terminal pads mounted ~2 cm away from the rosette terminals. These short jumper leads were intended to allow a finite cable displacement, thereby protecting the rosettes from damage, in case the terminal pad to which they were soldered was pulled accidentally during the trial.

A strain gauge insulation resistance tester was then used to carefully check individual grid resistances and overall rosette insulation resistances at the terminal pads, in the process confirming the integrity and labelling of the strain gauge cables. After this, the orientations of the strain gauges were carefully recorded and a liberal coat of opaque M-Coat D™ applied to the rosettes, jumper leads, bondable terminals and ends of the cabling. The contents of an M-Coat F™ kit were then used to maximise both water proofing and mechanical protection. Firstly, a soft sheet of Butyl rubber was pressed against the gauge installation to seal out moisture. Neoprene rubber sheets were then applied to provide protection against accidental impacts. Finally, a layer of aluminium tape was applied for maximum protection against flowing water with M-Coat B™ being used to seal around its edges. The strain gauge protection was concluded by securing the cabling to the vehicle using waterproof tape and cable-ties.

2.3. Strain Gauge Instrumentation

Each of the three individual grids of the strain gauge rosettes was connected up via Belden™ No. 8723 cable as a three-wire strain gauge to form a quarter-bridge of a Vishay™ model 2310 strain gauge amplifier. The four core cable was constructed of two twisted pairs, each of which was individually shielded. Such wire was used to maximise protection against electrostatic and electromagnetic interference (1). The amplifiers were set to a gain of 1000 and were also used to condition the signals by filtering out signals above 1 kHz. An eight channel Racal Vstore™ tape recorder recorded the conditioned signals on relatively inexpensive VHS video tapes. This unit was set to a 5 kHz bandwidth, and as well as having a combined voice log / data channel, also had a compensation channel which acted as a control during playback to compensate for tape flutter caused by shock loading. During the trial one channel became faulty, and data was only able to be recorded on six channels. Only two rosettes were therefore recorded for each run over the trial circuit. The recorder was mounted on an anti-shock isolation mount and surrounded by foam cushioning for the trial, as with the rest of the instrumentation in the vehicle. All instrumentation was powered by 240 volt AC power, obtained via an inverter from three 12 volt truck batteries.

2.4. Accelerometers

Acceleration measurements were also made at the front and back of the vehicle so that the stresses in the vehicle could be compared with ride severity. However, a complete acceleration-time history was only recorded for a few runs because of limited tape recorder channel capacity. The analysis of this data is not included in this report. Nevertheless, both accelerometers were monitored for all runs with an RMS Analyser on unfiltered mode which immediately determined the value of the RMS acceleration after each run. These RMS values gave a good estimate of the severity of the terrain and therefore a quick measure of the equivalence of repeated runs over the trial course. This is essential if the stresses for different rosettes, recorded on

separate runs of the vehicle around the test circuit, are to be compared meaningfully.

The accelerometers were of the piezoresistive type and were mounted beneath the drivers seat and at the base of the fuel tank filler neck at the rear of the vehicle. Both accelerometers were aligned to the vertical plane with a positive acceleration being towards the roof of the vehicle.

3. RESULTS AND ANALYSIS

3.1. Data Examination During Trial

The data output was monitored real time on an LCD display of the tape recorder during each run around the trial circuit. This ensured that a section of the circuit was immediately repeated if, for instance, a channel had over-ranged.

At the conclusion of each run, the test vehicle was halted and the data replayed on a oscillograph to check if the data was correctly recorded. A hard copy of the data was produced which also gave an overview of the strain gauge output to assist with later analysis.

	First Class Road (g)	Rough Course (g)	Second Class Road (g)	Cross-Country Course (g)
Front Accelerometer	0.94 (0.84-0.99)	—	1.08 (0.87-1.30)	0.97 (0.80-1.20)
Rear Accelerometer	0.12 (0.12-0.13)	0.50 (0.43-0.55)	0.13 (0.12-0.13)	0.22 (0.20-0.26)

Table 2: Mean and range (in parentheses) of RMS acceleration levels measured for each terrain type, where acceleration is given in 'g' (9.81 ms^{-2}).

3.3. Digital to Analogue Conversion

Unfortunately, the analogue to digital converter that was used to digitise the data for this preliminary analysis was originally designed for real-time digitisation of strain gauge signals and was only able to accept 64 kBytes per channel. This unfortunately limited the length of recording time that could be digitised in one record as it was important that a high enough digitisation rate was used so that enough data points could be acquired to sufficiently define the peaks and troughs of the strain-time history.

3.2. RMS Accelerations

Table 2 details the mean as well as the range of the root mean square (RMS) accelerations that were measured for each section of the trial circuit. No figures are given for the front accelerometer for the Ripple-Bar Rough Course as the peak acceleration values for this section often exceeded the limits of the RMS Analyser ($\sim 10 \text{ g}$), causing the RMS acceleration to be underestimated. The front of the vehicle experienced much higher accelerations than at the vehicle rear. The greatest stresses may therefore be expected in the front of the vehicle structure when the Rough Course is negotiated.

The RMS accelerations were, in general, relatively constant for the first three sections of the circuit, with the ride severity of the Second Class Road only increasing to a high value on a rainy day (RMS accelerations of 1.25 and 1.30). A notable exception was the Cross-Country Course where the track was broken up over the course of the trial leading to a gradual increase in ride severity.

According to Nyquist theory a time history must be digitised at twice the frequency of the highest frequency of interest so this latter frequency can be detected (2), but in order to fully characterise the peaks and troughs of a signal, greater sampling rates are required. For instance, a 1 kHz sampling rate is sufficient to characterise signals which have components of $\sim 100 \text{ Hz}$. This digitisation frequency was therefore used for the preliminary analyses of this paper.

In order to provide a meaningful comparison of the stresses at the various rosette locations, the data for the same obstacles of each section of the trial circuit were digitised.

Samples of 8 s length were taken from the First Class Road data, beginning at a location where engine braking commenced on a right-hand bend. Samples of 16 s length were taken for the Rough Course, Second Class Road and Cross-Country Courses. The samples for the latter two courses were taken in the vicinity of specific series of bumps that could be readily identified from the strain-time history.

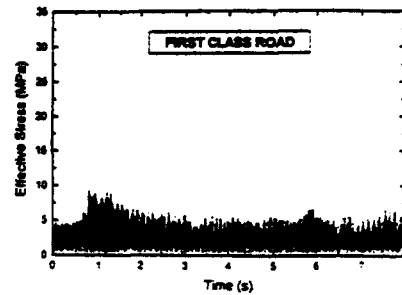
When the biaxial strain gauge data was converted into principal stresses, it was found that there were marked variations in the principal angle with stress at many rosette locations. The vehicle structure simply behaved in a nonlinear manner at these positions because it was subjected to a combination of non-proportional stresses. All digitised data was therefore converted into effective stress (3), the uniaxial equivalent of the measured biaxial stress state. As well as being readily interpretable, such data can be used to drive servo-hydraulic fatigue testing machines.

Fig. 4 shows examples of the stress-time histories experienced by Rosette C over the trial course. These are expressed as effective stresses which are always positive.

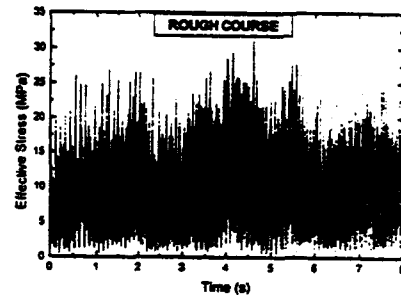
3.4. Measured Stresses

Table 3 compares the mean, RMS and maximum stresses at each of the rosette locations, for selected portions of the trial circuit. Table 4 summarises the stresses measured on the front glacis plate at various engine speeds when the vehicle was revved whilst stationary. RMS stresses are quoted in Tables 3 and 4 because they account for the variance of the stresses as well as their mean values.

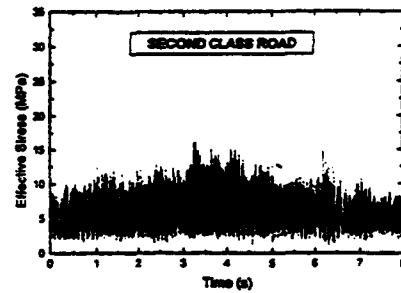
Significant stresses were developed in the front glacis plate because of engine braking (e.g. the sudden increase in stress at 0.75 s in Fig. 4(a)). This is probably related to vibrations from the booster units of the engine braking system being transmitted to the glacis plate. These booster units were bolted to mounting brackets which were welded to the inner-side of the glacis plate. The positions of the two mounting brackets are approximately defined, in Fig 3(b), by the lines joining Rosettes C and N as well as M and L, respectively.



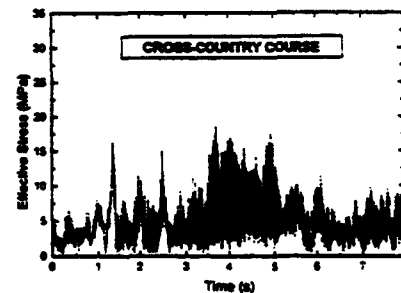
(a)



(b)



(c)



(d)

Figure 4: Effective stress-time plot for Rosette C: (a) First Class Road, (b) Rough Course, (c) Second Class Road, (d) Cross-Country Course.

Rosette C was positioned on the outer-side of the glasis plate, approximately 15 mm from the root of the weld that was used to fasten a mounting bracket onto the inner-side of the glasis plate. Rosettes N, M and L were positioned to evaluate the stresses at the other ends of the mounting brackets and were mounted at similar distances from the ends of the mounting brackets on the outer-side of the glasis plate as for Rosette C.

MEAN STRESS (MPa)				
Rosette	First Class	Rough Course	Second Class	Cross-Country
A	0.5	1.0	1.1	0.9
F	0.4	2.8	2.0	2.7
C	2.9	11	6.1	4.5
N	1.5	9.9	3.4	3.2
L	1.0	4.6	3.1	3.2
M	2.9	12.3	5.2	5.0

RMS STRESS (MPa)				
Rosette	First Class	Rough Course	Second Class	Cross-Country
A	0.7	1.1	1.1	1.1
F	0.8	3.3	2.2	3.5
C	3.2	12	7	5.4
N	1.8	11	4	3.8
L	1.1	5.1	3.3	4.2
M	3.4	15	6.1	6.4

MAXIMUM STRESS (MPa)				
Rosette	First Class	Rough Course	Second Class	Cross-Country
A	3.4	4.2	4.0	4.5
F	2.5	8.2	6.3	11
C	11	31	16	24
N	7.1	30	13	17
L	2.9	16	11	41
M	11	71	21	49

Table 3: Effective stresses measured for select portions of the trial circuit.

MEAN STRESS (MPa)			
Rosette	700 rpm	1700 rpm	700-3000 rpm
C	1.0	1.8	2.6
N	0.6	0.8	1.4
L	0.9	0.9	0.9
M	1.3	1.7	1.7

RMS STRESS (MPa)			
Rosette	700 rpm	1700 rpm	700-3000 rpm
C	1.0	1.9	2.8
N	0.7	1.0	1.5
L	1.0	0.9	1.0
M	1.4	1.9	2.0

MAXIMUM STRESS (MPa)			
Rosette	700 rpm	1700 rpm	700-3000 rpm
C	3.8	5.1	8.7
N	2.6	4.3	3.8
L	2.6	2.6	3.0
M	4.0	5.3	8.6

Table 4: Effective stresses measured at various engine speeds while the test vehicle was stationary, where engine speed is given in the common engineering unit of revolutions per minute (rpm).

3.5. Noise Spikes

A visual inspection of the strain-time data showed that spikes regularly occurred simultaneously on all channels at a frequency just over 100 Hz. Note that these spikes are not visible in Fig. 4. An FFT of a sample data set confirmed this frequency to be 109 Hz. While these spikes were first thought to be noise associated with the switching of the DC-AC inverter that powered the instrumentation in the vehicle, the strain gauge amplifiers may also have caused the problem. The particular amplifiers that were used, have in the past been found to exhibit similar noise spikes when used at high gains in quarter-bridge configurations, as with the current stress measurements. While the noise spikes were not

considered to lead to significant errors in the statistical data in Tables 3 and 4 they will in any case be filtered out before the data is used to drive servo-hydraulic testing machines.

4. DISCUSSION

While the mean and RMS stresses in Table 3 and 4 appear insignificant, the collated data is still a meaningful way to compare the severity of the stresses at the various strain gauge locations for the different terrain types. In any case, the maximum stress tables show the actual stress levels that can typically be reached for each experimental condition.

Table 3 shows that Rosettes C and M, mounted at the base of the brackets of the brake booster units, have the greatest response. The highest stresses are found in the Rough and the Cross-Country Courses, the Rough Course being the most severe as expected. In comparison, Rosettes A and F on the caps of the Shock absorber towers experience much lower stresses. Note that Rosettes A and F experience similar stresses on both the Rough and Cross-Country Courses whereas the glasis plate rosettes experience their greatest stresses on the Rough Course. The maximum stresses for Rosettes L and M in the Cross-Country Course are probably somewhat high as the data sample was recorded when the front of the vehicle hull was accidentally slammed into the side of a wheel rut. This is a rather severe loading case as stresses from the terrain are normally imparted to the vehicle structure via the vehicle suspension.

Table 4 summarises the stresses measured on the front glasis plate when the vehicle was revved whilst stationary. The table shows the stresses produced by constant engine speeds of 700 and 1700 rpm. Greater stresses still, were developed when the engine was run between 700 and 3000 rpm. Rosettes C and M were found to have the highest stresses with significant stresses being measured when running between 700 and 3000 rpm. In general, it appears that stresses associated with engine operation are an important component of the loads on the front glasis plate. The stresses associated with the operation of the engine braking system are also important as shown by the sudden increase in stress when engine braking commenced (e.g. 0.75 s in Fig. 4(a)).

Overall, the measured dynamic stresses are low in comparison to the material yield stress (nominally 1590 MPa) and would not normally be expected to cause fatigue cracking problems. However, cracking may possibly develop in conditions where there are high residual stresses and/or yield stress reductions caused by welding of the high hardness plate during vehicle fabrication. This is especially the case where a corrosive environment is present which may result in a potential for stress corrosion cracking. The stress measurements outlined in this paper will allow the fatigue and stress corrosion susceptibility of the high hardness armour to be determined using typical in-service loads.

5. CONCLUSION

An examination of the stress-time data from field testing of an LAV-25 vehicle revealed particular locations that are relatively highly stressed. The dynamic structural stresses in the vehicle can be related to the terrain traversed as well as vibration associated with engine operation and braking. Overall, the measured stress-time histories will provide the dynamic stress data essential for a correct laboratory simulation of the service environment.

6. ACKNOWLEDGMENTS

These stress measurements were conducted as a collaborative project with the Armoured Fighting Vehicles Group of the Australian Army Engineering Development Establishment (EDE), which also provided an LAV-25 vehicle and the use of their proving ground facilities at Monegeetta. Special thanks must go to Mr George Bettiol of the Development Laboratory, EDE, for co-ordinating the trial and arranging electronic instrumentation. Thanks must also go to Dr Ray Woodward of MRL for initiating the project.

7. REFERENCES

- (1) "Strain Gage Installation and Protection in Field Environments" Measurements Group, Inc., Technical Tip 607, 1983.
- (2) Press, W. H., *et al.* "Numerical Recipes - The Art of Scientific Computing" Cambridge University Press, New York, 1986, p. 381.
- (3) Dieter, G.E. "Mechanical Metallurgy", McGraw-Hill, Tokyo, 1981, p. 89.